Remaining useful life prediction for two-phase degradation model based on reparameterized inverse Gaussian process

Liangliang Zhuang[a], Ancha Xu[a,b,*], Yijun Wang[a], Yincai Tang[c]

[a] *School of Statistics and Mathematics, Zhejiang Gongshang University, Zhejiang 310018, China*
[b] *Collaborative Innovation Center of Statistical Data Engineering, Technology & Application Zhejiang Gongshang University, Zhejiang, China*
[c] *The KLATASDS-MOE, School of Statistics, East China Normal University, Shanghai 200241, China*

Abstract

Two-phase degradation is a prevalent degradation mechanism observed in modern systems, typically characterized by a change in the degradation rate or trend of a system's performance at a specific time point. Ignoring this change in degradation models can lead to considerable biases in predicting the remaining useful life (RUL) of the system, and potentially leading to inappropriate condition-based maintenance decisions. To address this issue, we propose a novel two-phase degradation model based on a reparameterized inverse Gaussian process. The model considers variations in both change points and model parameters among different systems to account for subject-to-subject heterogeneity. The unknown parameters are estimated using both maximum likelihood and Bayesian approaches. Additionally, we propose an adaptive replacement policy based on the distribution of RUL. By sequentially obtaining new degradation data, we dynamically update the estimation of model parameters and of the RUL distribution, allowing for adaptive replacement policies. A simulation study is conducted to assess the performance of our methodologies. Finally, a Lithium-ion battery example is provided to validate the proposed model and adaptive replacement policy. Technical details and additional results of case study are available as online supplementary materials.

Keywords: Reliability; adaptive replacement; maintenance; inverse Gaussian process; remaining useful life.

*Corresponding author
Email address: xuancha@mail.zjgsu.edu.cn (Ancha Xu)

1. Introduction

With the advancement of sensor technologies, prognostics and health management (PHM) has emerged as a critical topic in modern reliability engineering. Its primary objective is to enhance the safety and performance of systems. The increasing interest in PHM is evident in its application across various domains such as nuclear plants, electronics, and fleet industrial maintenance (Ye and Xie, 2015). The systematic approach of PHM involves monitoring the health status of systems, predicting the progression of failures, and minimizing operational risks through timely repair or replacement. Effective prognostics, which can provide early warnings of impending system failures, are crucial for implementing preventive actions, and thus can extend the lifespan of the system (Kordestani et al., 2023).

Degradation models play a pivotal role in PHM by furnishing invaluable insights into the progressive decline of a system's performance characteristic (PC) over time. These models encapsulate degradation paths that mirror the deterioration trajectory of PC, often established on the foundation of either physical principles or empirical understanding of the degradation process. Notably, linear, exponential, or power law degradation paths frequently serve as effective tools to characterize these degradation processes (Fang et al., 2022). However, these degradation paths assume a constant degradation mechanism for system performance, thereby overlooking the patterns of two-phase degradation. For example, the capacity of Lithium-ion batteries, as noted in Pop et al. (2005), often follow a two-phase degradation pattern throughout their lifespans: initially, the capacities degrade gradually, but after a certain number of charging cycles, degradation accelerates significantly. A similar degradation pattern emerges in ball bearing wear (Wen et al., 2018), and organic light-emitting diode luminosity (Wang et al., 2018a). As highlighted in Xiao et al. (2021), relying on single-pattern-based degradation models may inadequately fit the two-phase degradation data, resulting in imprecise predictions of remaining useful life (RUL) and potentially leading to improper maintenance decisions.

Introducing change points becomes essential to mark the transitions between these two-phase degradation patterns (Bae et al., 2016). To enhance the accuracy of estimating the lifetime distribution for systems with two-phase degradation paths, the general path and stochastic process-based two-phase degradation models have been proposed by researchers. In the general path models, Bae and Kvam (2004) introduced a random-coefficients model to elucidate the non-monotonic behavior of light display degradation across both burn-in and stable phases. Additionally, Chen and Tsui (2013) introduced a two-phase model to monitor

the degradation of rotational bearings and estimate RUL. They used a Bayesian framework, seamlessly combining historical and in-situ observations, to provide accurate predictions. In the realm of stochastic process modeling, a significant amount of research has concentrated on leveraging the Wiener process to encapsulate two-phase degradation processes (Gao et al., 2020; Ma et al., 2023). For example, Wang et al. (2018a) proposed a Wiener process model with measurement errors and change points, designed to fit degradation paths displaying a two-phase pattern using Bayesian method. Yan et al. (2021) proposed a two-phase physics-based Wiener process model, taking into account fatigue crack mechanisms and other factors. More recently, Wang et al. (2023a) proposed a prognosis-driven multi-threshold inspection and replacement model for two-phase Wiener degradation. The Wiener process is capable of representing non-monotonic degradation paths, making it useful for specific datasets. However, when dealing with monotonic degradation data, such as wear in power-shift steering transmission (Song and Cui, 2022), and operating current of Gallium arsenide laser (Zhou et al., 2024), the gamma and inverse Gaussian (IG) processes emerge as more suitable options. These processes empower researchers to effectively analyze degradation patterns and accurately estimate RULs for systems displaying monotonic degradation behavior.

To the best of our knowledge, only a limited number of studies have delved into the utilization of the two-phase gamma process model. For instance, Ling et al. (2019) proposed a two-phase degradation model under the gamma process, and employed both Bayesian and maximum likelihood (ML) methods to estimate unknown model parameters. Similarly, Lin et al. (2021) presented a fixed change-point two-phase gamma process model to analyze the voltage-discharge curves of battery aging under constant current. On the other hand, only Duan and Wang (2017) studied the two-phase IG degradation and employed the ML approach for estimating unknown parameters. While this paper pioneers the modeling of the two-phase IG degradation process, it remains subject to several limitations:

1. **Constraints on locations of change points**: In a two-phase degradation model with a change point (τ), illustrated in Figure 1(a), $Y(t)$ adheres to an IG process $\mathcal{IG}(\mu_1 t, \eta t^2)$ prior to time τ, and transitions to another IG process $\mathcal{IG}(\mu_2 t, \eta t^2)$ after τ. Assume that $t_j < \tau < t_{j+1}$, and denote that Y_j, Y_τ and Y_{j+1} are the degradation values at the time t_j, τ and t_{j+1}, respectively. The degradation increment $Y_{j+1} - Y_j$ can be decomposed into two distinct sub-increments: $Y_{j+1} - Y_\tau$ and $Y_\tau - Y_j$. It is established that $Y_{j+1} - Y_\tau \sim IG(a, b)$ and $Y_\tau - Y_j \sim IG(c, d)$, where $a = \mu_2(t_{j+1} - \tau)$, $b = \eta(t_{j+1} - \tau)^2$, $c = \mu_1(\tau - t_j)$, and $d = \eta(\tau - t_j)^2$. The probability density function

(PDF) of $IG(a, b)$ is

$$f_{IG}(x|a, b) = \sqrt{\frac{b}{2\pi x^3}} \exp\left\{-\frac{b(x-a)^2}{2a^2 x}\right\}. \tag{1}$$

Nevertheless, deriving the distribution of $Y_{j+1} - Y_j$ is challenging due to the non-additive nature of the defined IG distribution (1), even when $\mu_1 = \mu_2$. To circumvent this issue, Duan and Wang (2017) presumed that the change point coincides with the inspection time point, i.e., $\tau = t_j$ or $\tau = t_{j+1}$, simplifying the problem. However, in practical scenarios where change points are often random, rendering the assumption that τ aligns with inspection points is liable to introduce biases in parameter estimation, inaccuracies in RUL prediction, and suboptimal maintenance decisions.

2. **Insufficient considerations for deriving the lifetime distribution**. Duan and Wang (2017) treated the degradation state at the change point as a fixed value, subsequently deriving the distribution of failure time. Nonetheless, the estimation of the change point inherently involves information from the sample, and the uncertainty stemming from this estimation can propagate to the degradation state. Consequently, it becomes imperative to account for the uncertainty of the degradation state at the change point and to deduce the marginal distribution of failure time. Furthermore, their work omits consideration of important aspects such as RUL prediction and subsequent maintenance decisions.

3. **Neglecting the uncertainty in estimation**: Duan and Wang (2017) primarily employed the ML approach for point estimation in their two-phase model, without explicitly addressing the uncertainty inherent in the estimated parameters. Recognizing and addressing parameter uncertainty is a fundamental aspect of statistical inference, as it offers insights into the variability of the estimates. Particularly in scenarios characterized by limited sample sizes, estimators' variances tend to be substantial. Incorporating uncertainty quantification, such as interval estimation, becomes especially valuable in shedding light on key quantities of interest, such as mean-time-to-failure (MTTF), reliability, quantile lifetime, etc. Such uncertainty quantification proves invaluable for informed maintenance decisions (Wu et al., 2023; Xu et al., 2024).

To address the aforementioned limitations, we have undertaken substantial extensions. The main contributions and innovations of this paper are as follows:

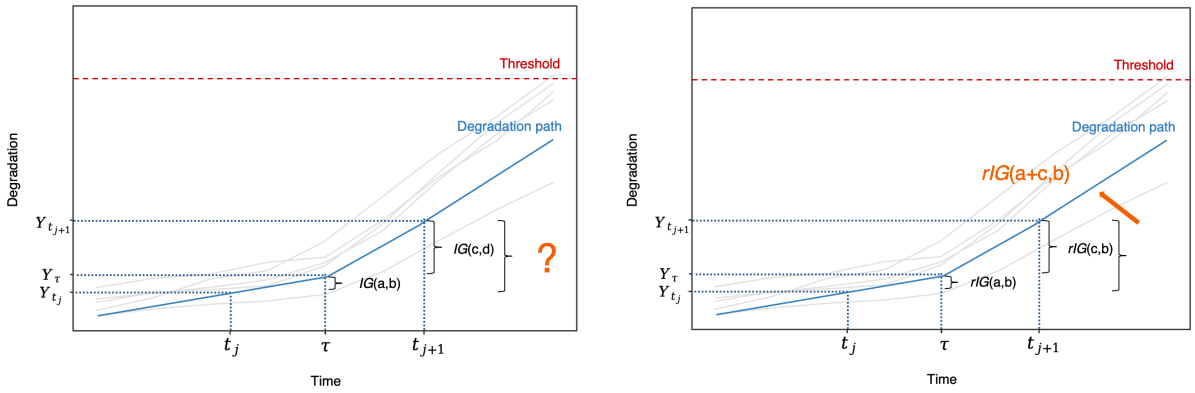

(a) IG process (b) Reparameterized IG process

Figure 1: Two types of two-phase stochastic processes.

1. A novel two-phase reparameterized IG (rIG) degradation model is developed to address the non-additivity challenge inherent in the traditional two-phase IG degradation model. Illustrated in Figure 1(b), when the change point falls within the time interval (t_j, t_{j+1}), we derive the distribution of the degradation increment $Y_{j+1} - Y_j$ based on the distributions of the two distinct sub-increments $Y_{j+1} - Y_\tau$ and $Y_\tau - Y_j$. Specifically, if $Y_{j+1} - Y_\tau \sim rIG(a, b)$ and $Y_\tau - Y_j \sim rIG(c, b)$, then $Y_{j+1} - Y_j \sim rIG(a + c, b)$. Details on the definition and properties of the rIG distribution will be presented in Section 2. In this innovative two-phase model, the change point is not confined to inspection time points; it can occur at any time. This expanded flexibility ensures that the new two-phase degradation model accommodates change points at arbitrary moments, providing a more accurate representation of complex degradation patterns.

2. We introduce distinct change points and model parameters for each individual system to address the inherent heterogeneity among devices. By acknowledging the uncertainty surrounding the degradation state at the change point, we derive the distribution of failure time and RUL for each system. We offer engineers two statistical inference methods to accurately identify change points and quantify parameter uncertainties: i) ML-based parameter estimation with interval estimates obtained through the parametric bootstrap method. ii) Bayesian approach utilizing adaptive rejection Metropolis sampling (ARMS)-Gibbs sampling to generate posterior samples and establish credible intervals. These intervals serve to convey the uncertainty associated with parameter estimates and RUL predictions, offering a comprehensive representation of the overall

uncertainty.

3. An adaptive replacement policy based on the distribution of RUL is proposed. While research on two/multi-phase degradation maintenance policies has garnered considerable attention, often optimizing decision variables based on fixed change points and minimizing cost rates (Zhang et al., 2024b; Yang et al., 2017), there is limited focus on unknown parameters and change point detection. Some studies, such as Fouladirad and Grall (2011); Fouladirad et al. (2008); Grall and Fouladirad (2008), address delayed change point detection with known model parameters. In contrast, our approach assumes unknown parameters (including change points) and dynamically updates them based on continuously acquired data. This adaptive policy aligns better with practical applications, enhancing the effectiveness of maintenance decisions amidst evolving system dynamics.

The rest of this paper is organized as follows. Section 2 introduces a two-phase rIG degradation model and derives the corresponding distributions of failure time and RUL. Section 3 presents the ML and Bayesian methods for estimating unknown model parameters and change points. A RUL-based adaptive replacement policy is proposed in Section 4. Section 5 conducts simulation studies to compare the inferential performance of ML and Bayesian methods. Section 6 carries out a case study to validate the proposed methodology. Finally, we summarize our findings in Section 7.

2. Two-phase reparameterized IG degradation model

In this section, we define the rIG process, apply it to the two-phase degradation model, and subsequently present the system failure time and RUL distribution.

2.1. The rIG process

Considerable research has been dedicated to modeling constant degradation mechanisms using the conventional IG process (Fan et al., 2024; Hao et al., 2019; Pan et al., 2016). However, the inapplicability of the additivity property of the conventional IG process poses a challenge when dealing with a two-phase degradation problem directly. To overcome this challenge, we first introduce the rIG distribution $rIG(\delta, \gamma)$, which forms the basis for our proposed rIG process. The parameter relationship between $rIG(\delta, \gamma)$ and the traditional

IG distribution $IG(a,b)$ is $a=\delta/\gamma$ and $b=\delta^2$ (Barndorff-Nielsen and Koudou, 1998). The PDF of $rIG(\delta,\gamma)$ is

$$f_{rIG}(y|\delta,\gamma)=\frac{\delta}{\sqrt{2\pi}}e^{\delta\gamma}y^{-3/2}e^{-\left(\delta^2y^{-1}+\gamma^2y\right)/2},\ y>0,\ \delta>0,\ \gamma>0, \tag{2}$$

and the cumulative distribution function (CDF) is

$$F_{rIG}(y|\delta,\gamma)=\Phi\left[\sqrt{y}\gamma-\frac{\delta}{\sqrt{y}}\right]+e^{2\delta\gamma}\Phi\left[-\sqrt{y}\gamma-\frac{\delta}{\sqrt{y}}\right], \tag{3}$$

where $\Phi(\cdot)$ is the CDF of the standard normal distribution. If a random variable Y follows the rIG distribution $rIG(\delta,\gamma)$, then the moment generating function (MGF) of Y is

$$M_Y(t)=E(e^{ty})=e^{\delta\gamma\left(1-\sqrt{1-\frac{2t}{\gamma^2}}\right)}. \tag{4}$$

According to (4), we know that the rIG distribution has additive property. That is, if $Y_1\sim rIG\left(\delta_1,\gamma\right)$ and $Y_2\sim rIG\left(\delta_2,\gamma\right)$, then $Y_1+Y_2\sim rIG\left(\delta_1+\delta_2,\gamma\right)$. The proof of (4) and the additive property can be found in Supplementary Section S1.

Based on rIG distribution, we provide the definition of the rIG process. A stochastic process $\{Z(t),t\geq 0\}$ is called rIG process if it satisfies: i) $Z(0)=0$ with probability one; ii) $Z(t)$ has independent increments. Specifically, $Z\left(t_2\right)-Z\left(t_1\right)$ and $Z\left(s_2\right)-Z\left(s_1\right)$ are independent for all $t_2>t_1\geq s_2>s_1\geq 0$; iii) For all $t>s\geq 0$, $Z(t)-Z(s)$ follows the rIG distribution $rIG\left(\delta(\Lambda(t)-\Lambda(s)),\gamma\right)$, where $\Lambda(t)$ is a monotone increasing function with $\Lambda(0)=0$, δ and γ are unknown parameters. We denote the rIG process $\{Z(t),t\geq 0\}$ as $r\mathcal{IG}\left(\delta\Lambda(t),\gamma\right)$, where δ is the drift parameter and γ is the dispersion parameter. Then from (4), we can derive the mean and variance of $\{Z(t),t\geq 0\}$, which are $\delta\Lambda(t)/\gamma$ and $\delta\Lambda(t)/\gamma^3$, respectively.

2.2. Two-phase rIG degradation model

Suppose the degradation of a system's PC unfolds across two distinct phases, marked by a single change point. The degeneration patterns in these two phases are assumed to conform to the rIG process, each characterized by a distinct drift to capture the differing degradation behavior before and after the change point. Moreover, the dispersion parameter γ is assumed to remain uniform across different systems, as it reflects the underlying failure mechanism of the system. Given that the sampled systems are drawn from the same population, it's commonly assumed that the failure mechanisms across various systems are

consistent. This assumption aligns with established practices in reliability analysis (Meeker et al., 2022; Zhai et al., 2024). We adopt a rIG-process-based degradation model that employs a linear function (i.e., $\Lambda(t) = t$). This choice aligns with the general practice of employing linear degradation models to characterize processes where the degradation rate increases linearly over time (Kong et al., 2017; Wang et al., 2018a). Furthermore, it is important to recognize that diverse systems might exhibit individualized change points. To account for this variability, we consider the change point, denoted as τ, as a random variable following a Gaussian distribution with a PDF of $g_\tau(\cdot|\mu_\tau, \sigma_\tau^2)$. This approach accommodates the inherent unit-to-unit variability. The adoption of a normal distribution assumption not only facilitates mathematical derivations but also offers analytical solutions for estimating μ_τ and σ_τ^2, making it a prevalent choice in the realm of degradation modeling (Lu et al., 2021; Shen et al., 2018). Thus, the proposed two-phase rIG degradation model is formulated as

$$\begin{aligned} &Y(t)|\tau \sim r\mathcal{IG}\left(m(t;\delta_1,\delta_2,\tau),\gamma\right),\ \tau \sim N\left(\mu_\tau,\sigma_\tau^2\right), \\ &m(t;\delta_1,\delta_2,\tau) = \begin{cases} \delta_1 t, & t \le \tau, \\ \delta_2\left(t-\tau\right)+\delta_1\tau, & t > \tau, \end{cases} \end{aligned} \tag{5}$$

where δ_1 and δ_2 are the drift parameters for $t \le \tau$ and $t > \tau$, respectively.

2.3. Failure-time and RUL

Using the two-phase rIG degradation model (5), we can derive the distributions of failure time and RUL for the systems. These derivations, as presented in the subsequent two theorems, hold significant importance for making informed maintenance decisions and optimizing the allocation of resources.

The failure time T is defined as the first passage time at which the degradation value $Y(t)$ of the system exceeds the failure threshold $\mathcal{D}$, represented as $T = \inf\{t \mid Y(t) \ge \mathcal{D}\}$. The reliability function of T and the MTTF of the system can be computed as follows.

Theorem 1. *The reliability function of T is*

$$\begin{aligned} R(t) &= P\left(Y(t) < \mathcal{D}, \tau \ge t\right) + P\left(Y(t) < \mathcal{D}, 0 < \tau < t\right) \\ &= \bar{F}_1\left(t \mid \tau\right)\bar{G}_\tau(t) + \int_0^t g_\tau(\tau|\mu_\tau,\sigma_\tau^2)\bar{F}_2\left(t \mid \tau\right)d\tau, \end{aligned} \tag{6}$$

where $\bar{G}_\tau(t)$ is the survival function of random variable τ, $\bar{F}_1(t|\tau) = P(T > t \mid \tau \ge t)$, and

$\bar{F}_2(t|\tau) = P(T > t \mid \tau < t)$. *Given the reliability function, the MTTF can be computed as*

$$MTTF = E(T) = \int_0^\infty R(t)dt. \tag{7}$$

Let y_t be the observed degradation value at time t. The RUL of the system at time t is defined as $S_t = \inf\{x; Y(t+x) \geq \mathcal{D} \mid Y_t < \mathcal{D}\}$. We have the following results.

Theorem 2. *The reliability function of RUL is*

$$R_{S_t}(x) = \bar{F}_{S_t,1}(x \mid \tau)\,\bar{G}_\tau(x+t) + \int_t^{x+t} g_\tau(\tau|\mu_\tau, \sigma_\tau^2)\bar{F}_{S_t,2}(x \mid \tau)\,d\tau + \int_0^t g_\tau(\tau)\bar{F}_{S_t,3}(x \mid \tau)\,d\tau, \tag{8}$$

where $\bar{F}_{S_t,i}, i = 1, 2, 3$ denotes the conditional reliability functions of S_t, arising from various relationships among times t, $t+x$, and τ. The PDF of RUL function can be computed by

$$f_{S_t}(x) = -\frac{\partial R_{S_t}(x)}{\partial x}. \tag{9}$$

The mean of RUL at time t can be obtained by

$$MRL = E(S_t) = \int_0^\infty R_{S_t}(x)dx. \tag{10}$$

The proofs of theorems 1 and 2 are given in Supplementary Section S2.

3. Statistical inference

In this section, considering unobserved change points, we present two methods to estimate both parameters and change points. Section 3.1 introduces the ML method, utilizing the expectation-maximization (EM) algorithm with the bootstrap method. Section 3.2 employs a Bayesian approach to quantify uncertainties in model parameters.

Assume there are a total of I systems under inspection in a degradation test. The degradation process of the i-th system encompasses a change point denoted as τ_i. The deterioration pattern of a system's PC follows the two-phase rIG degradation model (5). Denote $Y_{i,j}$ as the observed degradation value at the measurement time $t_{i,j}$, $i = 1\ldots, I$, $j = 1, \ldots, n_i$, and $0 < t_{i,1} < \ldots < t_{i,n_i}$. Let $\Delta y_{i,j} = Y_{i,j} - Y_{i,j-1}$, where $Y_{i,0} = 0$, and denote that $\boldsymbol{\Delta Y}_i = (\Delta y_{i,1}, \ldots, \Delta y_{i,n_i})^\top$, $\boldsymbol{\Delta Y} = \left(\boldsymbol{\Delta Y}_1^\top, \cdots, \boldsymbol{\Delta Y}_I^\top\right)^\top$. The distribution of $\Delta y_{i,j}$ can be determined based on the location of the change point τ_i. As shown in Figure 2, there are three potential scenarios for the change point τ_i. We denote these scenarios as $k = 1, 2$, and

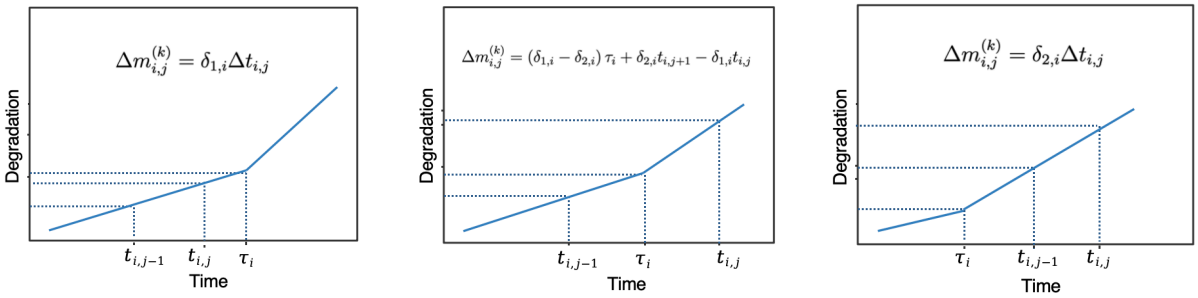

(a) $\tau_i \geq t_{i,j}$ (b) $t_{i,j-1} \leq \tau_i < t_{i,j}$ (c) $\tau_i < t_{i,j-1}$

Figure 2: Three scenarios for change points and inspection time.

3, corresponding to $\tau_i \geq t_{i,j}, t_{i,j-1} \leq \tau_i < t_{i,j}$, and $\tau_i < t_{i,j-1}$, respectively. Consequently, the distribution of $\Delta y_{i,j}$ can be expressed as $rIG\left(\Delta m_{i,j}^{(k)}\left(\delta_{1,i}, \delta_{2,i}, \tau_i\right), \gamma\right)$, where

$$\Delta m_{i,j}^{(k)}\left(\delta_{1,i}, \delta_{2,i}, \tau_i\right) = \begin{cases} \delta_{1,i}\Delta t_{i,j} & k = 1, \\ \left(\delta_{1,i} - \delta_{2,i}\right)\tau_i + \delta_{2,i}t_{i,j} - \delta_{1,i}t_{i,j-1}, & k = 2, \\ \delta_{2,i}\Delta t_{i,j}, & k = 3, \end{cases}$$

where $\Delta t_{i,j} = t_{i,j} - t_{i,j-1}$ and $t_{i,0} = 0$, $i = 1 \ldots, I$, $j = 1, \ldots, n_i$. For simplicity, let $\lambda_{i,j}^{(1)} = \mathcal{I}\left(\tau_i \geq t_{i,j}\right), \lambda_{i,j}^{(2)} = \mathcal{I}\left(t_{i,j-1} \leq \tau_i < t_{i,j}\right)$, and $\lambda_{i,j}^{(3)} = \mathcal{I}\left(\tau_i < t_{i,j-1}\right)$, then we have

$$\Delta m_{i,j}\left(\delta_{1,i}, \delta_{2,i}, \tau_i\right) = \Delta m_{i,j}^{(1)}\left(\delta_{1,i}, \delta_{2,i}, \tau_i\right)^{\lambda_{i,j}^{(1)}} \times \Delta m_{i,j}^{(2)}\left(\delta_{1,i}, \delta_{2,i}, \tau_i\right)^{\lambda_{i,j}^{(2)}} \times \Delta m_{i,j}^{(3)}\left(\delta_{1,i}, \delta_{2,i}, \tau_i\right)^{\lambda_{i,j}^{(3)}}.$$

Thus, given τ_i, the conditional PDF of $\Delta y_{i,j}$ can be written as

$$\begin{aligned} f_{i,j}\left(\Delta y_{i,j} \mid \delta_{1,i}, \delta_{2,i}, \tau_i, \gamma\right) = & \frac{\Delta m_{i,j}\left(\delta_{1,i}, \delta_{2,i}, \tau_i\right)}{\sqrt{2\pi}} \exp\left\{\gamma \Delta m_{i,j}\left(\delta_{1,i}, \delta_{2,i}, \tau_i\right)\right\} \Delta y_{i,j}^{-3/2} \\ & \times \exp\left\{-\frac{\left[\Delta m_{i,j}\left(\delta_{1,i}, \delta_{2,i}, \tau_i\right)\right]^2 \Delta y_{i,j}^{-1} + \gamma^2 \Delta y_{i,j}}{2}\right\}. \end{aligned} \tag{11}$$

Let $\boldsymbol{\delta}_1 = (\delta_{1,1}, \ldots, \delta_{1,I})^\top$, $\boldsymbol{\delta}_2 = (\delta_{2,1}, \ldots, \delta_{2,I})^\top$ and $\boldsymbol{\tau} = (\tau_1, \ldots, \tau_I)^\top$. Further, we denote $\boldsymbol{\eta} = \left(\boldsymbol{\delta}_1^\top, \boldsymbol{\delta}_2^\top, \gamma\right)^\top$, $\boldsymbol{\theta}_\tau = (\mu_\tau, \sigma_\tau^2)^\top$ and $\boldsymbol{\vartheta} = \left(\boldsymbol{\theta}_\tau^\top, \boldsymbol{\eta}^\top\right)^\top$. Given the observed data $\boldsymbol{\Delta Y}$, the likelihood function of the model parameters $\boldsymbol{\vartheta}$ is

$$L_{obs}(\boldsymbol{\Delta Y}|\boldsymbol{\vartheta}) = \prod_{i=1}^{I} \int_{-\infty}^{\infty} \prod_{j=1}^{n_i} f_{i,j}\left(\Delta y_{i,j} \mid \delta_{1,i}, \delta_{2,i}, \tau_i, \gamma\right) g_\tau(\tau_i|\boldsymbol{\theta}_\tau) \mathrm{d}\tau_i. \tag{12}$$

It is evident that obtaining a closed-form solution for the ML estimates (MLEs) of $\boldsymbol{\vartheta}$ is not feasible (Shao and Wang, 2023). To address challenges, we propose an EM algorithm, an

iterative optimization method primarily used for dealing with scenarios involving unobserved data, commonly applied in reliability analysis (Xiao et al., 2023; Wang et al., 2023b). This algorithm iteratively performs expectation step (E-step) and maximization step (M-step) to optimize model parameters.

3.1. EM algorithm with bootstrap method

We begin with the E-step, where we construct a Q-function representing the expected value of the complete log-likelihood for $(\boldsymbol{\Delta Y}, \boldsymbol{\tau})$. This expectation is calculated based on the conditional distribution of $\boldsymbol{\tau}$ given parameter vector $\boldsymbol{\vartheta}$. Next, in the M-step, we update the parameter estimates $\boldsymbol{\vartheta}$ by maximizing the expected log-likelihood obtained in the E-step. This iterative process continues until the specified convergence precision is achieved. The complete log-likelihood for $\boldsymbol{\tau}$ is expressed as:

$$l_c(\boldsymbol{\Delta Y}, \boldsymbol{\tau}|\boldsymbol{\vartheta}) = \sum_{i=1}^{I} l_i\left(\boldsymbol{\theta}_\tau\right) + \sum_{i=1}^{I}\sum_{j=1}^{n_i} l_{i,j}(\boldsymbol{\eta}, \boldsymbol{\tau}), \tag{13}$$

where

$$\begin{aligned} l_i\left(\boldsymbol{\theta}_\tau\right) &= \log g_\tau\left(\tau_i \mid \boldsymbol{\theta}_\tau\right) = -\log\sqrt{2\pi}\sigma_\tau - \frac{\left(\tau_i - \mu_\tau\right)^2}{2\sigma_\tau^2}, \\ l_{i,j}(\boldsymbol{\eta}, \boldsymbol{\tau}) &= \log f_{i,j}\left(\Delta y_{i,j} \mid \boldsymbol{\eta}, \boldsymbol{\tau}\right) \\ &= -\log\sqrt{2\pi} + \log\Delta m_{i,j} + \gamma\Delta m_{i,j} - \frac{3}{2}\log\Delta y_{i,j} - \frac{\Delta m_{i,j}^2}{2\Delta y_{i,j}} - \frac{\gamma^2\Delta y_{i,j}}{2}, \end{aligned}$$

and $\Delta m_{i,j} = \Delta m_{i,j}\left(\delta_{1,i}, \delta_{2,i}, \tau_i\right)$. Assuming that the optimal solution in the M-step during the s-th iteration is denoted as $\boldsymbol{\vartheta}_{(s)}$, in the subsequent $(s+1)$-th iteration, the initial step involves computing the following Q-function within the E-step:

$$\begin{aligned} \boldsymbol{Q}_{(s)}(\boldsymbol{\vartheta}) &= E_{\boldsymbol{\vartheta}_{(s)}}\left[l_c(\boldsymbol{\Delta Y}, \boldsymbol{\tau}|\boldsymbol{\vartheta})\right] \\ &= \sum_{i=1}^{I} E_{\boldsymbol{\vartheta}_{(s)}}\left[l_i\left(\boldsymbol{\theta}_\tau\right) \mid \boldsymbol{\Delta Y}\right] + \sum_{i=1}^{I}\sum_{j=1}^{n_i} E_{\boldsymbol{\vartheta}_{(s)}}\left[l_{i,j}(\boldsymbol{\eta}, \boldsymbol{\tau}) \mid \boldsymbol{\Delta Y}\right], \end{aligned} \tag{14}$$

which is the expectation of $l_c(\boldsymbol{\Delta Y}, \boldsymbol{\tau}|\boldsymbol{\vartheta})$ with respect to the conditional distribution of $\boldsymbol{\tau}$. The detailed derivation of two terms on the right-hand side of (14), $E_{\boldsymbol{\vartheta}_{(s)}}\left[l_i\left(\boldsymbol{\theta}_\tau\right) \mid \boldsymbol{\Delta y}\right]$ and $E_{\boldsymbol{\vartheta}_{(s)}}\left[l_{i,j}(\boldsymbol{\eta}, \boldsymbol{\tau}) \mid \boldsymbol{\Delta y}\right]$ can be found in supplementary material. Once the Q-function is obtained, we update the optimal solution in the M-step as

$$\boldsymbol{\vartheta}_{(s+1)} = \arg\max \boldsymbol{Q}_{(s)}(\boldsymbol{\vartheta}). \tag{15}$$

This can be accomplished through the utilization of numerical optimization algorithms, such as Newton or quasi-Newton algorithms, known for their quick convergence, memory efficiency, and applicability to high-dimensional nonlinear optimization (Jamshidian and Jennrich, 1997; Li et al., 2024). Consequently, the MLE of $\boldsymbol{\vartheta}$ can be computed iteratively until convergence is reached, and change points can be obtained by $E_{\hat{\boldsymbol{\vartheta}}}\{\tau_i \mid \boldsymbol{\Delta y}_i\}$, $i = 1, \ldots, I$. Technical details of the EM algorithm are available in Supplementary Section S3.

In addition to the point estimate $\boldsymbol{\vartheta}$, there is often a need to establish confidence intervals for a function of the parameters, denoted as $h(\boldsymbol{\vartheta})$. Constructing interval estimates is typically done using asymptotic theories. Nevertheless, given the intricacies of evaluating the Fisher information matrix for the proposed model, we opt for the parametric bootstrap method (Efron, 2012; Lamu and Yan, 2024) as an alternative approach to quantify the parameter uncertainty. The bootstrap procedure is outlined in Algorithm 1. After acquiring the bootstrap estimates $\left\{\hat{\boldsymbol{\vartheta}}_1^*, \ldots, \hat{\boldsymbol{\vartheta}}_{\mathcal{B}}^*\right\}$, we construct an approximate $100(1-\alpha)\%$ bootstrap confidence interval for a function of the parameters $h(\boldsymbol{\vartheta})$. The interval estimation is constructed as follows:

$$\left[h\left(\hat{\boldsymbol{\vartheta}}^*\right)_{(\alpha\mathcal{B}/2)}, h\left(\hat{\boldsymbol{\vartheta}}^*\right)_{((1-\alpha/2)\mathcal{B})}\right],$$

where $h\left(\hat{\boldsymbol{\vartheta}}^*\right)_{(b)}$ denotes the b-th statistic among $\left\{h\left(\hat{\boldsymbol{\vartheta}}^*\right)_1, \ldots, h\left(\hat{\boldsymbol{\vartheta}}^*\right)_{\mathcal{B}}\right\}$.

Algorithm 1: Parametric bootstrap algorithm.

Input: Point estimate $\hat{\boldsymbol{\vartheta}}$.

Output: $\mathcal{B}$ bootstrap estimates $\left\{\hat{\boldsymbol{\vartheta}}_1^*, \ldots, \hat{\boldsymbol{\vartheta}}_{\mathcal{B}}^*\right\}$.

```
for b = 1 to B do
    Generate τ from N(μ̂_τ, σ̂²_τ);
    for i = 1 to I do
        for j = 1 to n_i do
            Generate degradation sample ΔỸ_{i,j} from
             rIG(Δm^{(k)}_{i,j}(δ̂_{1,i}, δ̂_{2,i}, τ̂_i), γ̂), k = 1, 2, 3.
        end
    end
    Obtain ϑ̂*_b based on ΔỸ using the proposed EM algorithm.
end
```

3.2. Bayesian analysis

Bayesian analysis stands as a paramount methodology in the realm of PHM, celebrated for its distinctive capacity to harness prior knowledge and rigorously quantify the uncertainty of the unknown parameters (Taylor et al., 2024; Zhou et al., 2024). One of its primary advantages is the ability to incorporate existing information, often in the form of prior distributions, which encapsulate our prior beliefs about the parameters of interest. By integrating this prior knowledge with observed data, Bayesian analysis offers a powerful means to refine parameter estimates.

In this section, we utilize a Bayesian method to estimate the model parameters. The framework is set as follows:

$$Y_i(t|\tau_i) \sim r\mathcal{IG}\left(m(t;\delta_{1,i},\delta_{2,i},\tau_i),\gamma\right),\ \tau_i \sim N\left(\mu_\tau,\sigma_\tau^2\right),\ i=1,\ldots,I, \tag{16}$$

$$m(t;\delta_{1,i},\delta_{2,i},\tau_i) = \begin{cases} \delta_{1,i}t, & t \le \tau_i, \\ \delta_{2,i}\left(t-\tau_i\right)+\delta_{1,i}\tau_i, & t > \tau_i, \end{cases} \tag{17}$$

$$\left(\mu_\tau,\sigma_\tau^2\right) \sim NIGa\left(\beta_\tau,\eta_\tau,v_\tau,\xi_\tau\right),\gamma \sim N(\omega,\kappa^2), \tag{18}$$

$$\delta_{1,i} \sim N\left(\mu_1,\sigma_1^2\right),\delta_{2,i} \sim N\left(\mu_2,\sigma_2^2\right), \tag{19}$$

$$\left(\mu_1,\sigma_1^2\right) \sim NIGa\left(\beta_1,\eta_1,v_1,\xi_1\right),\left(\mu_2,\sigma_2^2\right) \sim NIGa\left(\beta_2,\eta_2,v_2,\xi_2\right), \tag{20}$$

where $NIGa(\cdot)$ denotes the normal-inverse gamma distribution. (16) and (17) are the model settings, consistent with Section 3.1. In (18), we establish priors for the shared parameters within the model. This enables us to improve the accuracy of τ_i estimation by incorporating information from other samples. Next, we provide a prior for the drift parameters. Due to potential variations in degradation paths among different systems, their drift parameters may differ. Nevertheless, considering commonalities among these systems as they belong to the same population, we adopt a hierarchical prior approach, transitioning from (19) to (20). This approach accommodates common effects and inherent unit-to-unit heterogeneity in the drift parameters, thereby capturing the rich complexity of degradation patterns across various systems.

Remark: Within the Bayesian framework, we allocate normal priors to the parameters γ, $\delta_{1,i}$, and $\delta_{2,i}$. While there exists a possibility that these parameters may take negative values, it is important to note that this probability becomes negligible when the ratio between the standard deviation and mean of the prior distribution is sufficiently small (Chen and Tsui, 2013; Wang et al., 2018b). This consideration aligns with common practice in Bayesian

modeling, where such cases of rare extreme values are often deemed inconsequential within a well-designed prior distribution. Furthermore, the choice of normal priors offers mathematical convenience and lends itself well to the establishment of hierarchical structures for hyperparameters. As highlighted in Bernardo and Smith (2009), the normal-inverse gamma distribution serves as the conjugate prior for the mean and variance parameters of the normal distribution. This property significantly streamlines the inference process, contributing to a more tractable and efficient analysis.

Let $\boldsymbol{\theta} = (\vartheta, \mu_1, \sigma_1^2, \mu_2, \sigma_2^2)^\top$ be the parameter vector in the two-phase model when we use the Bayesian model. According to Bayes' theorem, the joint posterior distribution of $\boldsymbol{\theta}$ can be derived as

$$\begin{aligned}\pi(\boldsymbol{\theta} \mid \boldsymbol{\Delta Y}) \propto \pi\left(\mu_\tau, \sigma_\tau^2\right) \pi\left(\mu_1, \sigma_1^2\right) \pi\left(\mu_2, \sigma_2^2\right) \pi\left(\gamma \mid \omega, \kappa\right) \pi\left(\tau \mid \mu_\tau, \sigma_\tau^2\right) \\ \times \pi\left(\boldsymbol{\delta}_1 \mid \mu_1, \sigma_1^2\right) \pi\left(\boldsymbol{\delta}_2 \mid \mu_1, \sigma_1^2\right) f_{\Delta Y}\left(\boldsymbol{\Delta Y} \mid \boldsymbol{\delta}_1, \boldsymbol{\delta}_2, \boldsymbol{\tau}, \gamma\right).\end{aligned} \tag{21}$$

Given the complexity of $\pi(\boldsymbol{\theta} \mid \boldsymbol{\Delta Y})$, a direct derivation of Bayesian estimates appears to be unfeasible. As an alternative, we employ the proposed sampling algorithm to generate posterior samples of the parameters (see Algorithm 2), where $\boldsymbol{\theta}_{\setminus\eta}$ denote the elements that remain within $\boldsymbol{\theta}$ after removing $\boldsymbol{\eta}$, thereby facilitating Bayesian inference. Their full conditional posterior distributions are given in Supplementary Section S4. Note that the full conditional posterior distributions of the parameters within $\boldsymbol{\theta}$, excluding $\boldsymbol{\tau}$, $\boldsymbol{\delta}_1$, and $\boldsymbol{\delta}_2$, are known distributions. As a result, their sample can be directly generated by statistical software. On the other hand, for τ_i, $\delta_{1,i}$, and $\delta_{2,i}$, where $i = 1, \ldots, I$, we must resort to the adaptive rejection Metropolis sampling (ARMS) algorithm (Gilks et al., 2022).

4. RUL-based adaptive replacement policy

In this section, we provide a detailed exposition of an adaptive replacement policy and establish a maintenance cost model that is grounded in the one-cycle criterion (Lu et al., 2022; Sheu et al., 2019), as discussed in Section 4.1. Section 4.2 will then focus extensively on evaluating the effectiveness and performance of the proposed policy, while also introducing two conventional policies for comparative analysis.

4.1. Adaptive replacement policy

Assume that the i-th system under consideration undergoes discrete inspection times denoted as $0 = t_{i,0} < t_{i,1} < \cdots < t_{i,j} < \cdots < t_{i,n_i}$. At each inspection time, $y_{i,j}$ represents

Algorithm 2: ARMS-Gibbs sampling algorithm.

Input: Observed data: $(\boldsymbol{\Delta Y}, \boldsymbol{\Delta t})$.

Output: The posterior samples of $\boldsymbol{\theta}$.

Set initial values $\boldsymbol{\theta}^{(0)} = \left(\boldsymbol{\vartheta}^{(0)}, \sigma_\tau^{2(0)}, \mu_1^{(0)}, \sigma_1^{2(0)}, \mu_2^{(0)}, \sigma_2^{2(0)}\right)^\top$.

for $s = 1$ **to** $\mathcal{S}$ **do**

  Generate posterior samples $\left(\mu_\tau^{(s)}, \sigma_\tau^{2(s)}\right)$, $\left(\mu_1^{(s)}, \sigma_1^{2(s)}\right)$ and $\left(\mu_2^{(s)}, \sigma_2^{2(s)}\right)$ of $(\mu_\tau, \sigma_\tau^2)$, (μ_1, σ_1^2), (μ_2, σ_2^2) from $NIGa\left(\beta_\tau'^{(s)}, \eta_\tau'^{(s)}, v_\tau'^{(s)}, \xi_\tau'^{(s)}\right)$, $NIGa\left(\beta_1'^{(s)}, \eta_1'^{(s)}, v_1'^{(s)}, \xi_1'^{(s)}\right)$ and $NIGa\left(\beta_2'^{(s)}, \eta_2'^{(s)}, v_2'^{(s)}, \xi_2'^{(s)}\right)$, respectively;

  Generate a posterior sample $\gamma^{(s)}$ of γ from $N(\omega', \kappa')$;

  Using ARMS algorithm to generate posterior samples $\delta_{1,i}^{(s)}$, $\delta_{2,i}^{(s)}$ and $\tau_i^{(s)}$ of $\delta_{1,i}$, $\delta_{2,i}$ and τ_i from $\pi\left(\delta_{1,i} \mid \boldsymbol{\theta}_{\setminus\delta_{1,i}}^{(s)}, \boldsymbol{\Delta y}\right)$, $\pi\left(\delta_{2,i} \mid \boldsymbol{\theta}_{\setminus\delta_{2,i}}^{(s)}, \boldsymbol{\Delta y}\right)$ and $\pi\left(\tau_i \mid \boldsymbol{\theta}_{\setminus\tau_i}^{(s)}, \boldsymbol{\Delta y}\right), i = 1, \ldots, I$, respectively.

end

The first $\mathcal{L}$ burn-in samples are discarded, and a total of $\mathcal{S} - \mathcal{L}$ posterior samples of each parameter are obtained. Based on these $\mathcal{S} - \mathcal{L}$ posterior samples, point and interval estimates are constructed.

the observed degradation value. The collection of degradation measurements is denoted as $y_{i,1:j} = \{y_{i,1}, y_{i,2}, \ldots, y_{i,j}\}$. Leveraging the parameter estimation techniques discussed in Section 3, we iteratively update the estimation of the model parameters and the RUL distribution, denoted as $f_{S_t}(x|y_{i,1:j})$, whenever new observations become available. This sequential updating process equips operators with real-time information to make dynamic maintenance decisions aimed at proactively preventing system failures. These dynamic maintenance decisions involve evaluating candidate maintenance actions at each inspection time point and determining optimal preparation and maintenance actions as data continues to be collected.

We assume that the failure is detected only by inspections, and the cost of each inspection is c_i. Maintenance is executed perfectly by replacing the system with brand-new identical spare parts. To ensure the reliability of the system, it is typically necessary to have an adequate supply of spare parts. Maintenance preparations are usually required to be ready before performing maintenance operations to avoid operational errors or unnecessary delays, including but not limited to preparing tools, equipment, technicians, and shutting down the system. This maintenance preparation time is denoted as ϖ.

This paper examines two maintenance actions: corrective replacement and preventive replacement. At inspection epoch $t_{i,j}$, when the system is operational, the decision maker has the option to choose between replacing the system preventively or waiting until the next inspection. Preventive replacement is implemented when it is expected that the system is nearing the failure state, incurring a preventive replacement cost denoted as c_p; in this case, upon the specified preparation time, the inspection is completed, followed by immediate repair upon preparation completion. If the system is found to fail during the inspection, it is then subject to corrective replacement, incurring a corrective replacement cost represented as c_c. Additionally, the downtime cost c_b associated with the preparation time subsequent to system failure must be taken into account. Therefore, at the current moment $t_{i,j}$, the candidate replacement time $\mathcal{T}_{i,j}$ of the i-th system can be achieved by minimizing the expected cost rate:

$$\begin{aligned}\mathcal{T}_{i,j} = \inf_{T_{i,j}} \Bigg\{ & \int_0^{T_{i,j}-t_{i,j}} \frac{c_c + c_i \lfloor x + t_{i,j} \rfloor + c_b}{x + t_{i,j} + \varpi} f_{S_t}(x|y_{i,1:j}) dx \\ & + \int_{T_{i,j}-t_{i,j}}^{+\infty} f_{S_t}(x|y_{i,1:j}) \frac{c_p + c_i \lfloor T_{i,j} - \varpi \rfloor}{T_{i,j}} dx \Bigg\},\end{aligned} \tag{22}$$

where $\lfloor \psi \rfloor = \max\{h \in \mathbb{Z} \mid t_{i,h} \leq \psi\}$ denotes the number of inspections before ψ. This involves assessing the trade-off between preventive replacement to avoid potential failures and the associated cost versus waiting until the next inspection for a more precise evaluation of the system's condition (Lu et al., 2022; Sheu et al., 2019). Note that $\mathcal{T}_{i,j}$ is considered a candidate value because long-term RUL prognostics may have lower accuracy. Fortunately, with the continuous collection of more inspection data, the proposed RUL-based adaptive replacement policy is expected to generate more precise prognostic results over time, allowing for the updating of the maintenance plan. As the values of $\mathcal{T}_{i,j}$ are successively updated, the optimal preparation time should be implemented for the first time when $\mathcal{T}_{i,j} - t_{i,j}$ equals or becomes less than ϖ. Once the preparation is completed, the replacement can be carried out. In other words, the optimal preparation time and the optimal replacement time are respectively given by:

$$\mathcal{T}_i' = \inf_{t_{i,j}} \{\mathcal{T}_{i,j} - t_{i,j} \leq \varpi\}, \quad \text{and} \quad \mathcal{T}_i^* = \mathcal{T}_i' + \varpi. \tag{23}$$

After the replacement, the newly installed component will resume operation, initiating a new maintenance decision-making process.

4.2. Performance evaluation and benchmark policies

We now shift our focus to evaluating the performance of the adaptive replacement policy. Consider a set of I systems, each of which operates for a single cycle. Let $\mathbb{X}_i = \min\{\mathcal{T}_i^*, \mathcal{T}_i^{\mathrm{f}}\}$, where $\mathcal{T}_i^*$ represents predicted optimal maintenance time, and $\mathcal{T}_i^{\mathrm{f}}$ represents actual failure time. At this point, the actual cost rate of the i-th system can be calculated by

$$CR_i = \begin{cases} \dfrac{c_p + c_i\lfloor \mathbb{X}_i - \varpi \rfloor}{\mathcal{T}_i^*}, & \mathbb{X}_i = \mathcal{T}_i^*, \\ \dfrac{c_c + c_i\lfloor \mathbb{X}_i \rfloor + c_b}{\mathcal{T}_i^{\mathrm{f}} + \varpi}, & \mathbb{X}_i = \mathcal{T}_i^{\mathrm{f}}. \end{cases} \tag{24}$$

The average cost rate for all systems is thus given by

$$\overline{CR} = \frac{\sum_{i=1}^{I} CR_i}{I}. \tag{25}$$

The data-driven dynamic adaptive replacement decision-making process is shown in Algorithm 3. We recommend using Bayesian methods for statistical inference in Algorithm 3 when implementing this replacement policy, as we find through simulation analysis in Section 5 that Bayesian method typically yields better performance compared to ML method. To highlight the superiority of the RUL-based adaptive replacement model, we also consider two simplified policies as benchmark maintenance policies. i). Classical replacement policy (CRP) that is based on historical reliability data. The preventive maintenance time is determined by the system's MTTF $\bar{\mathcal{T}}^F$. The cost rate of the i-th system is similar to (24), except that $\mathcal{T}_i^*$ is replaced by $\bar{\mathcal{T}}^F$, and does not consider the inspection cost. ii). Ideal replacement policy (IRP) that is based on the assumption of perfect predicted failure time $\mathcal{T}_i^P$. The cost rate of the i-th system is $c_p/\mathcal{T}_i^P$. Then, the average cost rate of all systems for both benchmark policies is calculated using (25).

5. Simulation study

This section gives simulation studies to investigate the performance of the proposed model and inference methods. We consider following three scenarios with different I and n_i: (I) $I = 5$ and $n_i = 20$; (II) $I = 5$ and $n_i = 40$; (III) $I = 8$ and $n_i = 20$. The dispersion parameter $\gamma = 2$. Considering the heterogeneity, we generate $\delta_{1,1}, \ldots, \delta_{1,I}$ from $N(4, 1)$, $\delta_{2,1}, \ldots, \delta_{2,I}$ from $N(15, 1)$, and $\tau_1, \ldots, \tau_I$ from $N(10, 1)$. For the i-th system, given the change point τ_i, the degradation increments are simulated from the rIG distribution (11). For each scenario, we generate 500 samples to reduce the effects of randomness on the results.

Algorithm 3: RUL-based adaptive replacement policy.

Input: $y, c_c, c_p, c_b, \varpi, \mathcal{D}, j$.

Output: $\mathcal{T}_i^*$, $CR_i, i = 1, \ldots, I$, and $\overline{CR}$.

for $i = 1$ **to** I **do**
  while *no maintenance performed* **do**
    if *the system is operational* **then**
      Collect new inspection data $Y_{i,j}$;
      Update model parameter estimates using Bayesian methods in Section 3;
      Compute RUL distribution $\{f_{S_t}(x|y_{i,1:j})\}_{x=0}^{+\infty}$ using (9);
      Determine $\mathcal{T}_{i,j}$ by (22), and find $\mathcal{T}_i'$ by (23);
      if $t_{i,j} = \mathcal{T}_i'$ **then**
        Inspection is completed, and preventive maintenance at $\mathcal{T}_i^*$.
      end
    end
    else
      Corrective maintenance;
      Set $\mathcal{T}_i^{\mathrm{f}} = t_{i,j}$.
    end
    $j = j + 1$.
  end
  Compute CR_i by (24).
end
Compute $\overline{CR}$ by (25).

5.1. Parameter estimation performance of two inference methods

First, we fit the simulated data using the proposed model and methods. For the Bayesian method, the posterior samples of $\boldsymbol{\theta}$ are generated via the ARMS-Gibbs algorithm in Section 3.2. We employ flat priors, where $(\mu_\tau, \sigma_\tau) \sim NIGa(8, 100, 0.01, 0.01)$, $(\mu_1, \sigma_1) \sim NIGa(1, 100, 0.01, 0.01)$, $(\mu_2, \sigma_2) \sim NIGa(2, 100, 0.01, 0.01)$, and $\gamma \sim N(5, 100)$. For each scenario, posterior samples are obtained after a burn-in period of $\mathcal{L} = 5000$ iterations, during which convergence is monitored using diagnostic tools. Following the burn-in phase, an additional $\mathcal{S} - \mathcal{L} = 5000$ iterations are conducted to obtain posterior samples for

subsequent inference, and posterior estimates for all parameters are calculated as the means of their corresponding samples. For the ML method, we determine the initial values for the estimates in the EM algorithm based on the estimates obtained from the Bayesian method. Point estimates are obtained using the EM algorithm from Section 3.1, while corresponding interval estimates are calculated using the parametric bootstrap method with $\mathcal{B} = 500$. The convergence of the EM algorithm is determined by the criterion $|\boldsymbol{\vartheta}(s+1) - \boldsymbol{\vartheta}(s)| < 10^{-3}$, where $|\cdot|$ representing the L_1 distance.

Table 1: Parameter estimation from Bayesian and ML methods for three scenarios.

Scen.	Meth.	Stat.	$\delta_{1,1}$	$\delta_{1,2}$	$\delta_{1,3}$	$\delta_{1,4}$	$\delta_{1,5}$	$\delta_{2,1}$	$\delta_{2,2}$	$\delta_{2,3}$	$\delta_{2,4}$	$\delta_{2,5}$	γ
I	Bayes	RB	0.024	0.029	-0.007	0.015	0.012	-0.026	0.019	0.023	0.056	0.003	0.011
		RMSE	1.326	1.363	1.357	1.332	1.330	0.422	0.424	0.476	0.422	0.431	0.168
		CP	0.956	0.953	0.946	0.953	0.957	0.941	0.925	0.900	0.928	0.926	0.964
	ML	RB	0.057	0.039	0.040	0.057	0.050	0.065	0.071	0.057	0.078	0.060	0.057
		RMSE	1.315	1.381	1.302	1.401	1.508	0.641	0.645	0.576	0.667	0.739	0.308
		CP	0.889	0.922	0.878	0.900	0.833	0.922	0.922	0.900	0.889	0.867	0.811
Scen.	Meth.	Stat.	$\delta_{1,1}$	$\delta_{1,2}$	$\delta_{1,3}$	$\delta_{1,4}$	$\delta_{1,5}$	$\delta_{2,1}$	$\delta_{2,2}$	$\delta_{2,3}$	$\delta_{2,4}$	$\delta_{2,5}$	γ
II	Bayes	RB	-0.005	0.007	0.023	0.011	-0.005	-0.019	0.000	0.016	0.000	0.012	0.001
		RMSE	1.068	1.011	1.065	1.015	1.044	0.349	0.283	0.275	0.355	0.332	0.124
		CP	0.930	0.945	0.950	0.944	0.927	0.902	0.925	0.947	0.885	0.902	0.914
	ML	RB	0.036	0.035	0.017	0.032	0.039	0.029	0.041	0.036	0.025	0.042	0.039
		RMSE	0.944	1.010	0.880	0.900	0.985	0.331	0.358	0.323	0.328	0.346	0.150
		CP	0.905	0.890	0.905	0.920	0.900	0.895	0.890	0.930	0.930	0.920	0.865
Scen.	Meth.	Stat.	$\delta_{1,1}$	$\delta_{1,2}$	$\delta_{1,3}$	$\delta_{1,4}$	$\delta_{1,5}$	$\delta_{1,6}$	$\delta_{1,7}$	$\delta_{1,8}$			
III	Bayes	RB	-0.024	-0.010	-0.004	-0.010	0.010	-0.002	0.015	0.029			
		RMSE	1.121	1.096	1.087	1.083	1.083	1.221	1.124	1.155			
		CP	0.946	0.953	0.942	0.951	0.947	0.911	0.943	0.940			
	ML	RB	0.089	0.073	0.086	0.079	0.066	0.076	0.074	0.073			
		RMSE	1.098	1.095	1.087	1.179	1.015	1.028	0.993	1.018			
		CP	0.887	0.900	0.913	0.880	0.887	0.887	0.867	0.893			
		Stat.	$\delta_{2,1}$	$\delta_{2,2}$	$\delta_{2,3}$	$\delta_{2,4}$	$\delta_{2,5}$	$\delta_{2,6}$	$\delta_{2,7}$	$\delta_{2,8}$	γ		
	Bayes	RB	0.011	-0.060	0.012	-0.073	0.030	-0.022	0.021	0.107	-0.001		
		RMSE	0.463	0.432	0.314	0.485	0.327	0.356	0.379	0.494	0.138		
		CP	0.915	0.909	0.977	0.916	0.960	0.931	0.947	0.918	0.946		
	ML	RB	0.087	0.095	0.087	0.085	0.102	0.070	0.087	0.097	0.091		
		RMSE	0.642	0.629	0.606	0.604	0.623	0.604	0.545	0.569	0.230		
		CP	0.880	0.887	0.893	0.887	0.873	0.900	0.920	0.900	0.893		

Table 1 displays the results of two inference methods, presenting relative bias (RB), root mean square error (RMSE), and 95% coverage probability (CP). For point estimation, both Bayesian and ML methods show small RBs and appropriate RMSEs. Notably, for scenarios I and II, the RMSE of both methods generally decreases with increasing n_i, as a larger number of measurements enhances accuracy. Comparatively, scenario III sees a modest reduction in RMSE due to the additional information from more systems, leading to more accurate parameter estimation. However, for interval estimation, the Bayesian approach significantly outperforms the ML method across all scenarios. This superiority is evident in the CPs obtained by the Bayesian approach, which are close to the nominal level of 0.95. In contrast, the CPs based on the ML method fall well below 0.95. Thus, we recommend employing the Bayesian method for parameter estimation.

5.2. Model comparison in reliability estimation

We conduct another simulation study to compare the superiority of the proposed models in reliability estimation. We consider scenarios I and III, assuming that system failures occur in the second phase, with a threshold set at 75. Several benchmark models are considered, which do not account for change points: a linear rIG model $\Lambda(t) = t$; two nonlinear models with the following forms of $\Lambda(t)$: i) power law $\Lambda(t;\alpha) = t^{\alpha}$, and ii) exponential law $\Lambda(t;\alpha) = \exp(\alpha t) - 1$. For these benchmarks, we employ Bayesian methods, assuming α follows a normal distribution $N(5, 100)$, where a large variance means weak prior information for the parameter α. The priors of other parameters remain consistent with these in section 5.1. Figure 3 presents the average RMSE results for the MTTF of various models. It can be observed that the results obtained by Bayesian method for the proposed model are smaller than those obtained by other models. This indicates the accuracy of our model in predicting system failures.

5.3. Change point estimation under real-time scenarios

To emphasize the superiority of the proposed model in real-time scenarios for change point detection, we conduct a new simulation based on scenario II ($n_i = 40$). Assuming the data is dynamically acquired, we perform parameter estimation based on the existing data $y_{i,1:j}$ and provide change point detection results. Figure 4 illustrates the average RMSE of change point estimates at $j = 20, 30$, and 40. As expected, the RMSEs decrease gradually with an increase in the amount of acquired data, and both methods exhibit very small

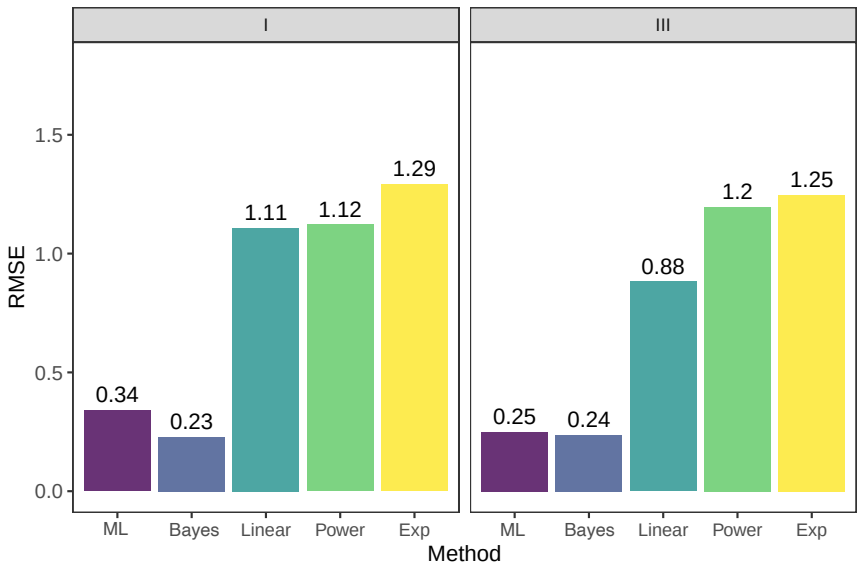

Figure 3: Average RMSE of MTTF estimators based on various models.

RMSEs, indicating accurate identification of change points. In comparison, the Bayesian method outperforms the ML approach, as it results in smaller RMSEs for each change point.

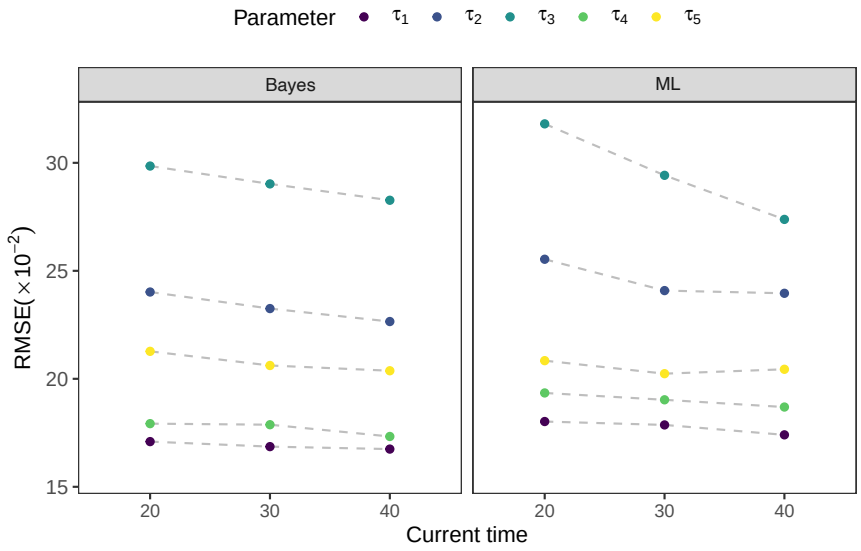

Figure 4: Average RMSE of the change point estimates at three different time points.

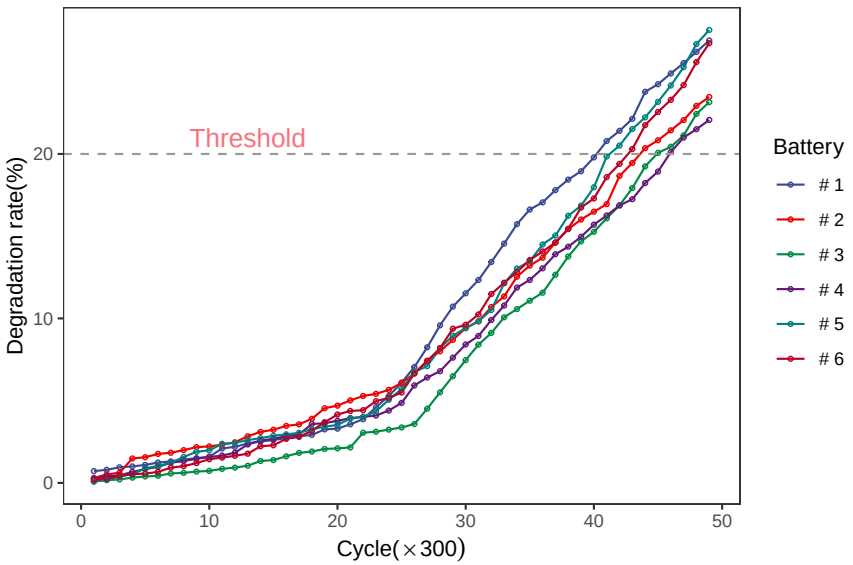

Figure 5: Capacity degradation data of 6 lithium batteries.

6. Case study

In this section, we demonstrate the proposed method using a dataset of lithium-ion battery degradation. Lithium-ion batteries are extensively employed in commercial products like mobile phones and electric vehicles. The failure of lithium-ion batteries can lead to reduced device performance and loss of functionality. Therefore, accurately predicting RUL distribution and delivering reliable maintenance actions are pivotal in ensuring the reliability and cost-effectiveness of equipment operation (Zhang et al., 2023; Peng et al., 2018).

Figure 5 displays degradation data for six battery capacity measurements, where "Cycle" represents one charging and discharging cycle of the battery. From Figure 5, we see that the capacity degradation of each battery exhibits a two-phase characteristic, with an initial phase showing a low degradation rate followed by a subsequent phase with a higher degradation rate. Based on this dataset, our objective is to use the proposed model to fit the degradation paths of these batteries and provide RUL prediction distributions (see Section 6.1). Following this, our objective is to extend the application to real-world scenarios and present the outcomes of the proposed adaptive replacement policy (see Section 6.2).

6.1. Parameter estimation

We fit the degradation dataset by the proposed two-phase rIG model. Both Bayesian and ML methods are used to estimate the parameters of the models. The settings for both

Table 2: The estimation of the parameters and change points based on the Bayesian and ML methods.

Battery		Bayesian method			ML method		
		$\boldsymbol{\beta}_1$	$\boldsymbol{\beta}_2$	$\boldsymbol{\tau}$	$\boldsymbol{\beta}_1$	$\boldsymbol{\beta}_2$	$\boldsymbol{\tau}$
# 1	2.5%	0.422	2.198	22.257	0.497	2.511	22.987
	Mean	0.536	2.437	23.187	0.510	2.632	23.011
	97.5%	0.645	2.851	24.664	0.518	2.713	23.032
# 2	2.5%	0.523	2.013	24.365	0.638	2.113	25.245
	Mean	0.608	2.356	25.336	0.658	2.215	25.321
	97.5%	0.785	2.615	26.557	0.670	2.282	25.398
# 3	2.5%	0.336	2.161	26.316	0.405	2.412	26.773
	Mean	0.468	2.424	26.761	0.414	2.531	26.801
	97.5%	0.518	2.831	27.381	0.420	2.610	26.821
# 4	2.5%	0.467	1.993	24.151	0.561	2.120	24.923
	Mean	0.569	2.345	25.008	0.576	2.221	24.971
	97.5%	0.703	2.595	26.060	0.587	2.288	25.025
# 5	2.5%	0.495	2.162	23.184	0.624	2.382	23.932
	Mean	0.588	2.418	23.893	0.642	2.496	23.940
	97.5%	0.752	2.809	25.370	0.654	2.572	23.944
# 6	2.5%	0.464	2.130	24.722	0.559	2.324	25.561
	Mean	0.566	2.408	25.576	0.574	2.440	25.625
	97.5%	0.697	2.769	26.306	0.585	2.517	25.667

methods are consistent with those used in the simulation experiments. To evaluate the convergence of the EM algorithm and the ARMS-Gibbs sampling algorithm, we present the iteration process of the parameters for the EM algorithm, as well as the trace plots and ergodic mean plots of the posterior samples in Supplementary Section S5. These plots demonstrate that both algorithms converge rapidly. The estimation of the parameters and change points are presented in Table 2. The γ estimates from the two methods (Bayesian and ML) are 2.930 and 3.001, respectively, with corresponding 95% credible (confidence) intervals: (2.615, 3.556) for Bayesian method, and (2.804, 3.165) for ML approach.

Moreover, to assess the prediction capability of the proposed model, we employ the first 30 data points to fit the model and predict the degradation rates for the last 19 cycles. As

a comparison, we consider the two-phase IG model (Duan and Wang, 2017), assuming that the change point occurs at the inspection time point, denoted as "Duan". The unknown parameters in their model are determined using the ML method. Since their method cannot directly detect change points, they additionally use the Schwarz information criterion to choose change points by balancing model fit and complexity. However, this method can only identify the change point at a specific inspection point. In contrast, the proposed model directly estimates change points with uncertainty that can occur at any time. Table 3 presents the RBs and RMSEs for training, prediction, and overall performance based on five models, where "Proposed" refers to our proposed model using the Bayesian approach for parameter estimation. From Table 3, it is evident that three models without considering change points perform poorly in predictions with high RMSE and RB values. As an example, we provide the fitted and predicted paths for battery #2 for each model in Figure 6. As we can see the model without considering change points performs poorly in fitting the data, rendering it challenging to make accurate predictions for future degradation paths. However, the two-phase models effectively identify the locations of change points and yield prediction values that closely align with the actual values. Compared to the "Duan" model, the proposed model demonstrates superior predictive performance, yielding lower RMSE and RB values. This improvement can be attributed to the proposed model's more accurate change point detection. As an illustrative example, we focus on the potential change point location for battery #2 in Figure 6. It is evident that the estimated change points based on the proposed model and the "Duan" model differ, and this discrepancy has implications for the estimation of the degradation rate in the second phase, ultimately affecting the accuracy of RUL predictions.

Next, based on the estimation results of the proposed model, we can derive the failure time and RUL distribution for each battery, as discussed in Section 2.3. Here, we take the Bayesian estimation as an example and present the reliability and density functions of the failure time for each battery using data from the first 30 cycles. The results are shown in Figure 7, with the threshold chosen as $\mathcal{D} = 20\%$. Based on (7), the MTTFs for each battery are 41.984, 43.208, 43.658, 44.588, 43.320, and 42.257, respectively. Figure 8 presents the reliability and density functions of RUL for different batteries at the current cycle (30-th), while the corresponding MRL are 9.352, 13.375, 14.354, 15.111, 13.180, and 11.925, respectively.

Table 3: RMSE and RB results for different models.

Model	Training		Prediciton		Overall	
	RMSE	RB	RMSE	RB	RMSE	RB
Proposed	0.448	0.248	1.538	0.060	1.020	0.175
Linear	3.476	1.442	3.685	0.156	3.558	0.943
Power	2.057	0.568	2.475	0.113	2.229	0.391
Exp	0.908	0.313	1.611	0.065	1.230	0.217
Duan	0.434	0.239	1.976	0.075	1.276	0.175

6.2. RUL-based adaptive maintenance policy

Based on the RUL prediction results, the proposed adaptive replacement policy can be employed to determine the optimal replacement time for each battery. To highlight the applicability of our proposed model in real-time scenarios, we consider the dataset from cycles 1 to 30 as historical data, continuously acquiring new data over time. In this case, both the estimates of the model parameters and the RUL distribution will be updated when a new observation is obtained. Using the expected cost rate (22), we can determine candidate replacement time for each battery during the continuous data collection period. For illustration purposes, the candidate replacement times for battery #2 and #3 are shown in Table 4, where $c_i = 2, c_c = 600, c_p = 200, c_b = 100$, and $\varpi = 1$. Furthermore, the table also includes the true RUL and predicted MRL. From Table 4, we can observe that the candidate replacement time is dynamically adjusted based on the RUL prediction. The optimal preparation time for batteries #2 and #3 are 42 and 43, respectively. Once the preparation is completed, the optimal replacement times are 43 and 44, respectively, which coincide with the corresponding failure time of the two batteries. This indicates that preventive maintenance should be performed for both batteries.

To highlight the impact of diagnostic accuracy on the adaptive maintenance policy, we compare the results of the proposed two-phase model with the previously mentioned models. Note that the "Duan" model assumes that the change point is given and does not give the derivation of RUL distribution. Thus, we only compare the proposed model with the other three models that do not consider change points (Linear, Power, Exp). Table 5 shows the optimal replacement times for 6 batteries under different models. Here, "FC"

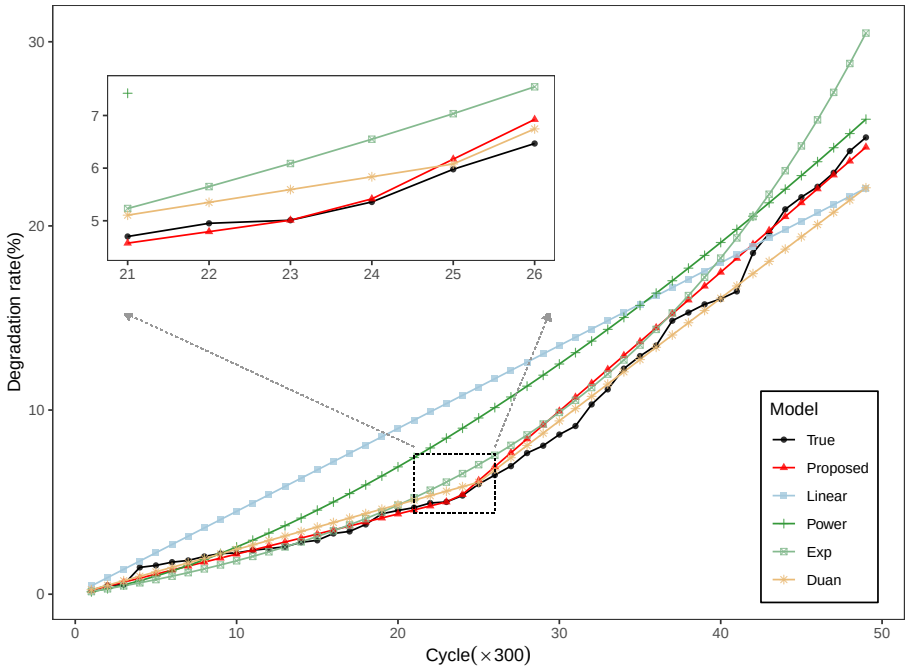

Figure 6: Degradation path training and prediction results for battery #2 using different methods, with a zoomed-in view of the potential change point locations.

refers to the true failure time for batteries, and "P" and "C" indicate that the maintenance actions are preventive and corrective maintenance, respectively. It can be seen from the table that under the adaptive replacement policy, except for the power model, which has five corrective maintenance actions, the final/optimal replacement time of all batteries in other models is less than FC, that is, P action is performed.

Figure 9 illustrates the average cost rate for each policy, where ARP represents our proposed adaptive replacement policy. The proposed two-phase rIG model under ARP is referred to as ARP-TP. It can be observed that, except for the ARP-Power policy, other RUL-based ARPs are significantly superior to CRP. Another noteworthy finding is that ARP-TP is closest to IRP, compared to other policies. The reduction in average cost rate based on ARP-TP may be attributed to the efficacy of our proposed two-phase model, which proficiently captures change point locations and precisely fits degradation paths.

7. Conclusion

In this study, we propose a novel two-phase rIG model to model monotonically degrading data with a change point. The model takes into account variations in both change points

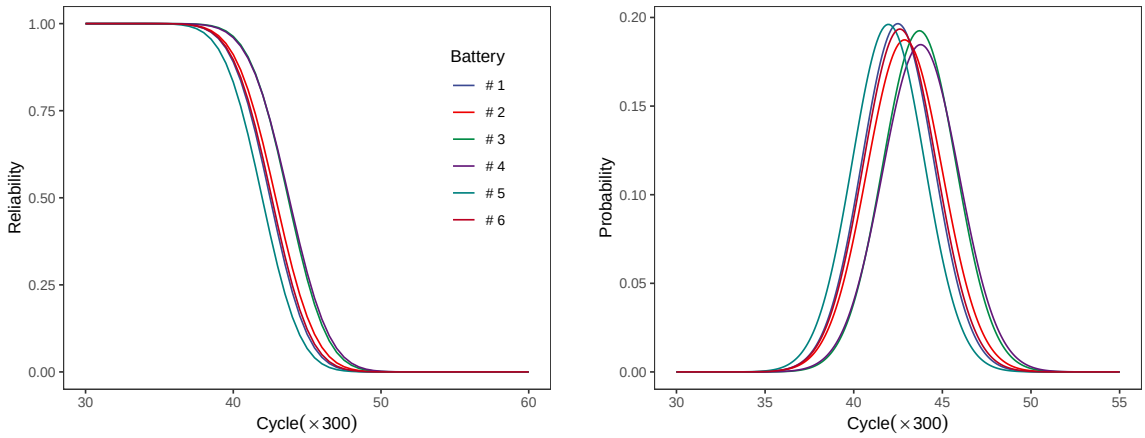

(a) (b)

Figure 7: Reliability and density functions of failure time based on Bayesian method.

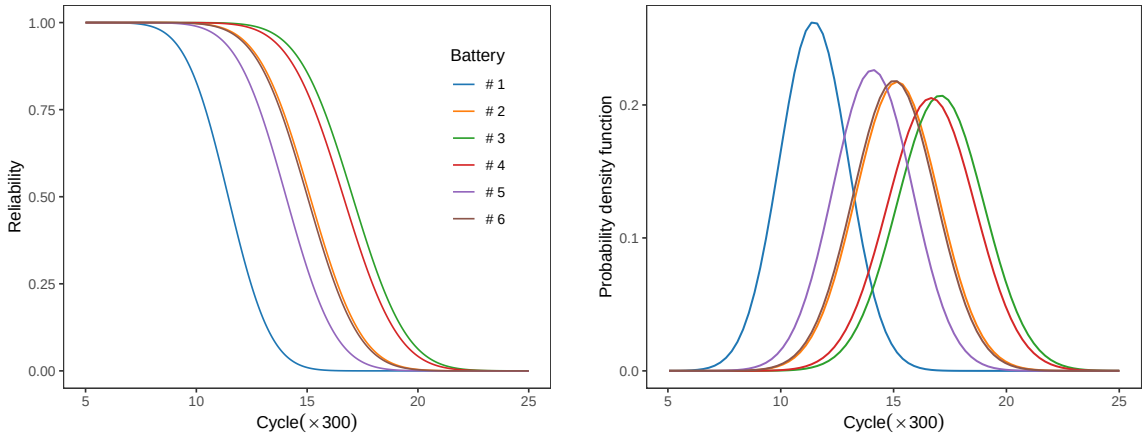

(a) (b)

Figure 8: Reliability and density functions of RUL based on Bayesian method at 30-th cycle.

and model parameters among different systems to address subject-to-subject heterogeneity. The failure time and RUL distributions for the two-phase rIG model are derived. We employ likelihood-based and Bayesian methods for parameter estimation to develop the EM and ARMS-Gibbs algorithms, respectively. In addition, we propose an adaptive replacement policy based on RUL distribution. Simulation studies are conducted to compare the performance of Bayesian and ML methods, as well as to compare the proposed model with other candidate models, across different scenarios. The results indicate that the Bayesian method outperforms the ML method in obtaining interval estimation, and the proposed model demonstrates accurate MTTF prediction compared to other models. Furthermore,

Table 4: Candidate replacement time for batteries #2 and #3 at consecutive data-acquisition epochs, with optimal preparation time of 42 and 43, respectively.

Cycle(×300)	Battery #2			Battery #3		
	Real RUL	MRL	$\mathcal{T}_{2,j}$	Real RUL	MRL	$\mathcal{T}_{3,j}$
31	12	13.865	43	13	13.228	46
33	10	11.219	41	11	10.278	43
35	8	7.624	41	9	8.389	42
37	6	5.986	41	7	6.884	42
39	4	4.040	42	5	4.206	43
41	2	2.764	43	3	2.318	44
42	1	1.235	43	2	1.556	44
43	-	-	-	1	0.380	44

we apply the proposed model to six battery datasets and compare it with several benchmark models. The results demonstrate that our model can accurately identify the locations of change points and fit the degradation paths of the batteries well. By continuously acquiring inspection data, we dynamically update the estimation of model parameters and RUL distributions, enabling adaptively adjusted replacement plans. Compared to other policies, we find that the proposed policy provides an accurate replacement time that is closer to the product failure time without exceeding its effective lifetime.

The paper preliminary explores an adaptive replacement policy to demonstrate the impact of model construction and RUL prediction on subsequent maintenance decisions. However, there are several potential areas that warrant further investigation. For instance, in scenarios where the change point has not yet occurred during the early stages of the degradation process, training a two-stage degradation model becomes challenging. Therefore, dynamic change point detection becomes crucial for effective decision-making and necessitates further exploration (Fan and Lu, 2020). Additionally, when a system exhibits dependencies across multiple PCs, a multivariate two-stage degradation model should be considered (Zhang et al., 2024a; Wu et al., 2020). This would involve more complex maintenance policies and require exploration into optimal strategies.

Table 5: Maintenance cost rates for 6 batteries under the adaptive replacement policy.

Battery	FC	Proposed			Linear			Power			Exp		
		$\mathcal{T}_i^*$	Action	CR	$\mathcal{T}_i^*$	Action	CR	$\mathcal{T}_i^*$	Action	CR	$\mathcal{T}_i^*$	Action	CR
1	40	37	P	7.351	37	P	7.351	40	P	6.950	35	P	7.657
2	43	43	P	6.605	42	P	6.714	-	C	17.909	40	P	6.950
3	44	44	P	6.500	44	P	6.500	-	C	17.556	42	P	6.714
4	45	44	P	6.500	43	P	6.605	-	C	17.217	41	P	6.829
5	41	40	P	6.950	39	P	7.077	-	C	18.667	38	P	7.211
6	42	42	P	6.714	41	P	6.829	-	C	18.326	40	P	6.950

Supplementary Materials

Supplementary document: (a) proof of the additivity of rIG distribution; (b) derivation of theorems 1 and 2; (c) technical details of the EM algorithm, including conditional expectations in the E-step, Q-function, and procedural steps; (d) technical details of the Bayesian analysis, containing full conditional posterior distribution; and (f) additional results of the case studies, including iterative results of model parameter estimation for Bayesian and ML methods.

Acknowledgments

The research is supported by Zhejiang Provincial Natural Science Foundation of China (LZ24A010002), Natural Science Foundation of China (12171432, 12101549, 12271168), the China Scholarship Council program (202308330508), the Fundamental Research Funds for the Provincial Universities of Zhejiang, the Summit Advancement Disciplines of Zhejiang Province (Zhejiang Gongshang University—Statistics), and Collaborative Innovation Center of Statistical Data Engineering Technology & Application.

References

Bae, S.J., Kvam, P.H., 2004. A nonlinear random-coefficients model for degradation testing. Technometrics 46, 460–469. doi:10.1198/004017004000000464.

Bae, S.J., Yuan, T., Kim, S.j., 2016. Bayesian degradation modeling for reliability prediction of organic light-emitting diodes. Journal of Computational Science 17, 117–125. doi:10.1016/j.jocs.2016.08.006.

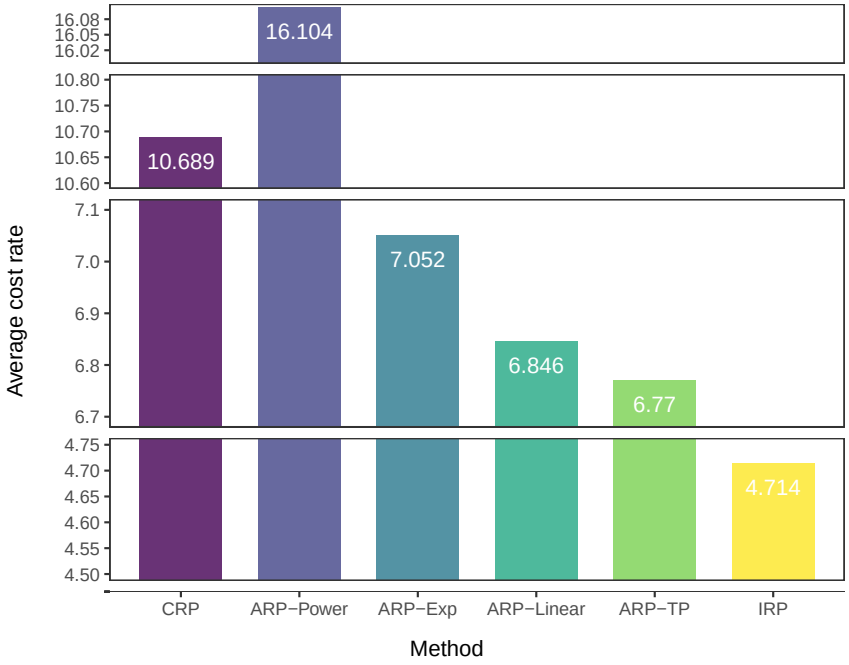

Figure 9: Average cost rate for each policy.

Barndorff-Nielsen, O.E., Koudou, A.E., 1998. Trees with random conductivities and the (reciprocal) inverse Gaussian distribution. Advances in Applied Probability 30, 409–424. doi:10.1239/aap/1035228076.

Bernardo, J.M., Smith, A.F., 2009. Bayesian Theory. John Wiley & Sons.

Chen, N., Tsui, K.L., 2013. Condition monitoring and remaining useful life prediction using degradation signals: revisited. IIE Transactions 45, 939–952. doi:10.1080/0740817x.2012.706376.

Duan, F., Wang, G., 2017. Reliability modeling of two-phase inverse gaussian degradation process, in: 2017 Second International Conference on Reliability Systems Engineering, IEEE. pp. 1–6. doi:10.1109/ICRSE.2017.8030736.

Efron, B., 2012. Bayesian inference and the parametric bootstrap. The annals of applied statistics 6, 1971. doi:10.1214/12-AOAS571.

Fan, T.H., Dong, Y.S., Peng, C.Y., 2024. A complete Bayesian degradation analysis based on inverse Gaussian processes. IEEE Transactions on Reliability 73, 536–548. doi:10.1109/TR.2023.3304673.

Fan, Y., Lu, X., 2020. An online Bayesian approach to change-point detection for categorical data. Knowledge-Based Systems 196, 105792. doi:10.1016/j.knosys.2020.105792.

Fang, G., Pan, R., Wang, Y., 2022. Inverse Gaussian processes with correlated random effects for multivariate degradation modeling. European Journal of Operational Research 300, 1177–1193. doi:10.1016/j.ejor.2021.10.04.

Fouladirad, M., Grall, A., 2011. Condition-based maintenance for a system subject to a non-homogeneous wear process with a wear rate transition. Reliability Engineering & System Safety 96, 611–618. doi:10.1016/j.ress.2010.12.008.

Fouladirad, M., Grall, A., Dieulle, L., 2008. On the use of on-line detection for maintenance of gradually deteriorating systems. Reliability Engineering & System Safety 93, 1814–1820. doi:10.1016/j.ress.2008.03.020.

Gao, H.D., Cui, L.R., Dong, Q.L., 2020. Reliability modeling for a two-phase degradation system with a change point based on a Wiener process. Reliability Engineering & System Safety 193, 106601. doi:10.1016/j.ress.2019.106601.

Gilks, W., Best, N., Tan, K., 2022. Adaptive rejection metropolis sampling within gibbs sampling. Applied Statistics 44, 455–472. doi:10.2307/2986138.

Grall, A., Fouladirad, M., 2008. Maintenance decision rule with embedded online Bayesian change detection for gradually non-stationary deteriorating systems. Proceedings of the Institution of Mechanical Engineers, Part O: Journal of Risk and Reliability 222, 359–369. doi:10.1243/1748006XJRR141.

Hao, S., Yang, J., Berenguer, C., 2019. Degradation analysis based on an extended inverse Gaussian process model with skew-normal random effects and measurement errors. Reliability Engineering & System Safety 189, 261–270. doi:10.1016/j.ress.2019.04.031.

Jamshidian, M., Jennrich, R.I., 1997. Acceleration of the EM algorithm by using quasi-Newton methods. Journal of the Royal Statistical Society: Series B (Statistical Methodology) 59, 569–587. doi:10.1111/1467-9868.00083.

Kong, D.J., Balakrishnan, N., Cui, L.R., 2017. Two-phase degradation process model with abrupt jump at change point governed by Wiener process. IEEE Transactions on Reliability 66, 1345–1360. doi:10.1109/Tr.2017.2711621.

Kordestani, M., Orchard, M.E., Khorasan, K., Saif, M., 2023. An overview of the state-of-the-art in aircraft prognostic and health management strategies. IEEE Transactions on Instrumentation and Measurement 72, 1–15. doi:10.1109/TIM.2023.3236342.

Lamu, D., Yan, R., 2024. Reliability estimation of s-out-of-k system with Kumaraswamy distribution based on partially constant stress accelerated life tests. Statistical Theory and Related Fields doi:10.1080/24754269.2024.2359826.

Li, X., Gao, Y., Chang, H., Huang, D., Ma, Y., Pan, R., Qi, H., Wang, F., Wu, S., Xu, K., et al., 2024. A selective review on statistical methods for massive data computation: distributed computing, subsampling, and minibatch techniques. Statistical Theory and Related Fields doi:10.1080/24754269.2024.2343151.

Lin, C.P., Ling, M.H., Cabrera, J., Yang, F., Yu, D.Y.W., Tsui, K.L., 2021. Prognostics for lithium-ion batteries using a two-phase gamma degradation process model. Reliability engineering & system safety 214, 107797. doi:10.1016/j.ress.2021.107797.

Ling, M.H., Ng, H.K.T., Tsui, K.L., 2019. Bayesian and likelihood inferences on remaining useful life in two-phase degradation models under gamma process. Reliability Engineering & System Safety 184, 77–85. doi:10.1016/j.ress.2017.11.017.

Lu, B., Chen, Z., Zhao, X., 2022. Data-driven dynamic adaptive replacement policy for units subject to heterogeneous degradation. Computers & Industrial Engineering 171, 108478. doi:10.1016/j.cie.2022.108478.

Lu, L., Wang, B., Hong, Y., Ye, Z., 2021. General path models for degradation data with multiple charac-

teristics and covariates. Technometrics 63, 354–369. doi:10.1080/00401706.2020.1796814.

Ma, J., Cai, L., Liao, G., Yin, H., Si, X., Zhang, P., 2023. A multi-phase Wiener process-based degradation model with imperfect maintenance activities. Reliability Engineering & System Safety 232. doi:10.1016/j.ress.2022.109075.

Meeker, W.Q., Escobar, L.A., Pascual, F.G., 2022. Statistical methods for reliability data. John Wiley & Sons.

Pan, D., Liu, J.B., Cao, J., 2016. Remaining useful life estimation using an inverse Gaussian degradation model. Neurocomputing 185, 64–72. doi:10.1016/j.neucom.2015.12.041.

Peng, W., Ye, Z.S., Chen, N., 2018. Joint online RUL prediction for multivariate deteriorating systems. IEEE Transactions on Industrial Informatics 15, 2870–2878. doi:10.1109/TII.2018.2869429.

Pop, V., Bergveld, H.J., Notten, P., Regtien, P.P., 2005. State-of-the-art of battery state-of-charge determination. Measurement Science and Technology 16, 93. doi:10.1088/0957-0233/16/12/R01.

Shao, J., Wang, X., 2023. MLE with datasets from populations having shared parameters. Statistical Theory and Related Fields 7, 213–222. doi:10.1080/24754269.2023.2180185.

Shen, L., Wang, Y., Zhai, Q., Tang, Y., 2018. Degradation modeling using stochastic processes with random initial degradation. IEEE Transactions on Reliability 68, 1320–1329. doi:10.1109/TR.2018.2885133.

Sheu, S.H., Tsai, H.N., Sheu, U.Y., Zhang, Z.G., 2019. Optimal replacement policies for a system based on a one-cycle criterion. Reliability Engineering & System Safety 191, 106527. doi:10.1016/j.ress.2019.106527.

Song, K., Cui, L., 2022. A common random effect induced bivariate gamma degradation process with application to remaining useful life prediction. Reliability Engineering & System Safety 219, 108200. doi:10.1016/j.ress.2021.108200.

Taylor, D., Rigdon, S.E., Pan, R., Montgomery, D.C., 2024. Bayesian D-optimal design for life testing with censoring. Quality and Reliability Engineering International 40, 71–90. doi:10.1002/qre.322.

Wang, J., Longyan, T., Ma, X., Gao, K., Jia, H., Yang, L., 2023a. Prognosis-driven reliability analysis and replacement policy optimization for two-phase continuous degradation. Reliability Engineering & System Safety 230, 108909. doi:10.1016/j.ress.2022.108909.

Wang, P., Tang, Y., Bae, S.J., Xu, A., 2018a. Bayesian approach for two-phase degradation data based on change-point Wiener process with measurement errors. IEEE Transactions on Reliability 67, 688–700. doi:10.1109/tr.2017.2785978.

Wang, P., Tang, Y., Joo Bae, S., He, Y., 2018b. Bayesian analysis of two-phase degradation data based on change-point Wiener process. Reliability Engineering & System Safety 170, 244–256. doi:10.1016/j.ress.2017.09.027.

Wang, Z., Zhai, Q., Shen, L., 2023b. Degradation modeling and RUL prediction in dynamic environments using a Wiener process with an autoregressive rate. IEEE Transactions on Reliability 73, 912–921. doi:10.1109/TR.2023.3319497.

Wen, Y., Wu, J., Das, D., Tseng, T.L., 2018. Degradation modeling and RUL prediction using Wiener process subject to multiple change points and unit heterogeneity. Reliability Engineering & System Safety 176, 113–124. doi:10.1016/j.ress.2018.04.005.

Wu, T., Yang, L., Ma, X., Zhang, Z., Zhao, Y., 2020. Dynamic maintenance strategy with iteratively

updated group information. Reliability Engineering & System Safety 197, 106820. doi:10.1016/j.ress.2020.106820.

Wu, W., Wang, B.X., Chen, J., Miao, J., Guan, Q., 2023. Interval estimation of the two-parameter exponential constant stress accelerated life test model under type-II censoring. Quality Technology & Quantitative Management 20, 751–762. doi:10.1080/16843703.2022.2147688.

Xiao, T., Park, C., Lin, C., Ouyang, L., Ma, Y., 2023. Hybrid reliability analysis with incomplete interval data based on adaptive Kriging. Reliability Engineering & System Safety 237, 109362. doi:10.1016/j.ress.2023.10936.

Xiao, X., Chen, P., Ye, Z., Tsui, K.L., 2021. On computing multiple change points for the gamma distribution. Journal of Quality Technology 53, 267–288. doi:10.1080/00224065.2020.1717398.

Xu, A., Wang, B., Zhu, D., Pang, J., Lian, X., 2024. Bayesian reliability assessment of permanent magnet brake under small sample size. IEEE Transactions on Reliability doi:10.1109/TR.2024.3381072.

Yan, B.X., Ma, X.B., Huang, G.F., Zhao, Y., 2021. Two-stage physics-based Wiener process models for online RUL prediction in field vibration data. Mechanical Systems and Signal Processing 152, 107378. doi:10.1016/j.ymssp.2020.107378.

Yang, L., Ma, X., Zhao, Y., 2017. A condition-based maintenance model for a three-state system subject to degradation and environmental shocks. Computers & Industrial Engineering 105, 210–222. doi:10.1016/j.cie.2017.01.012.

Ye, Z.S., Xie, M., 2015. Stochastic modelling and analysis of degradation for highly reliable products. Applied Stochastic Models in Business and Industry 31, 16–32. doi:10.1002/asmb.2063.

Zhai, Q., Ye, Z., Li, C., Revie, M., Dunson, D., 2024. Modeling recurrent failures on large directed networks. Journal of the American Statistical Association doi:10.1080/01621459.2024.2319897.

Zhang, W., Zhang, X., He, S., Zhao, X., He, Z., 2024a. Optimal condition-based maintenance policy for multi-component repairable systems with economic dependence in a finite-horizon. Reliability Engineering & System Safety 241, 109612. doi:10.1016/j.ress.2023.109612.

Zhang, Y., Feng, F., Wang, S., Meng, J., Xie, J., Ling, R., Yin, H., Zhang, K., Chai, Y., 2023. Joint nonlinear-drift-driven Wiener process-Markov chain degradation switching model for adaptive online predicting lithium-ion battery remaining useful life. Applied Energy 341, 121043. doi:10.1016/j.apenergy.2023.121043.

Zhang, Y., Ouyang, L., Meng, X., Zhu, X., 2024b. Condition-based maintenance considering imperfect inspection for a multi-state system subject to competing and hidden failures. Computers & Industrial Engineering 188, 109856. doi:10.1016/j.cie.2023.109856.

Zhou, S., Xu, A., Tang, Y., Shen, L., 2024. Fast bayesian inference of reparameterized gamma process with random effects. IEEE Transactions on Reliability 73, 399–412. doi:10.1109/TR.2023.3263940.